 CMES, vol.85, no.6, pp.481-498, 2012

Dual Hybrid Boundary Node Method for Solving Transient Dynamic Fracture Problems

Y. Miao[1], T.G. HE[1], H. Luo[1,2] and H.P. Zhu[1]

Abstract: Combined the hybrid boundary node method (Hybrid BNM) and the dual reciprocity principle, a truly boundary-type meshless method, namely, dual hybrid boundary node method (Dual Hybrid BNM) is presented for solving transient dynamic fracture problems. The enriched basis functions in moving least squares (MLS) approximation is presented for simulating the singularity of the stress field on the tip of the fracture. The solution in Dual Hybrid BNM is divided into particular solution and complementary solution. The complementary solution is solved by means of Hybrid BNM, and the particular solution is approximated by using radial basis functions (RBF). The inner nodes are just for RBF interpolation, which is not influence that the present method is a boundary-only method. The present method has many advantages such as simple pre-process and higher accuracy. Numerical examples have shown the validity of the presented scheme.

Keywords: Dual reciprocity method, Hybrid boundary node method, Dynamic fracture problems, Enriched basis function.

1 Introduction

Classical finite element method (FEM) for dynamic fracture propagation simulation is limited because of the use of mesh. Fracture propagation requires an update of the mesh during the computation, which can become a real challenge in 3D, particularly for dynamic fracture propagation. Some techniques can avoid using a mesh and are particularly adapt to crack propagation, i.e., extended finite element method (XFEM) [Moës, Dolbow, and Belytschko (1999); Dolbow, Moës, and Belytschko (2000); Moës and Belytschko (2002)], which introduces local enrichment functions in the FEM approximation in order to represent the discontinuity of the displacement across the crack lines. A second way is the boundary

[1] School of Civil Engineering and Mechanics, Huazhong University of Science and Technology, Wuhan 430074, China

[2] Corresponding Author. Tel: 86 27 87559534; Fax: 86 27 87542231; H. Luo Email: autumn_luoh@163.com

element method [Budreck and Achenbach (1988); Hirose and Achenbach (1989); Gallego and Dominguez (1996); Dominguez and Gallego (1992)], which permits to simulate the propagation simply by adding new boundary elements along crack extension. The third one is the meshless methods [Belytschko, Lu, and Gu (1994); Liu and Gu (2001); Atluri and Zhu (1998); Mukherjee and Mukherjee (1997)], which let the cracks propagate among a set of nodes. The hybrid boundary node method (Hybrid BNM) [Zhang and Yao (2001); Zhang, Yao, and Li (2002); Zhang and Yao (2004); Miao, Wang, and Yu (2005); Miao and Wang (2006)], which is a boundary-type meshless method, is used in this paper to solve transient dynamic fracture problems.

The Hybrid BNM is proposed as a truly boundary-type meshless method, which does not require a 'boundary element mesh', either for the purpose of interpolation of the solution variables or for the integration of 'energy'. It has several advantages, such as, it completely avoid 'meshing' so that the preprocess will become quite easy compared with those methods based on 'mesh', and also the 'remeshing' during the analysis of crack propagation can be avoided. The dimension of problem can be reduced as using BEM, which constitute one of the best alternatives for the solution of crack problems. The computed stress and displacement fields are very accurate and the modeling effort is reduced to its minimum since only the crack surfaces need to be discretized besides any external boundary.

The Hybrid BNM, however, can only be used for solving homogeneous problems. For the dynamic fracture problems, the domain integration is inevitable. The Dual reciprocity method (DRM) was first proposed by Nardini and Brebbia (1983) for elasto-dynamic problems. Based on Hybrid BNM, DRM is first introduced into Hybrid BNM by Miao, Wang, and Wang (2009), and a new truly meshless method named Dual Hybrid Boundary Node Method (Dual Hybrid BNM) is proposed, which can be applied to dynamic problem, nonlinear problem and so on.

In the present paper, the Dual Hybrid BNM is used to solve the dynamic fracture problems. In order to simulate the singularity of the stress on the tip of crack, enriched basis functions [Rao and Rahman (2004); Li and Cheng (2005)] are used. Because of the complexity of complete basis functions, we use local basis functions instead, which can offer a lower computation cost and an accurate simulating of the stress state on the crack tip.

In the following paragraphs, the formulations of Dual Hybrid BNM for elastodynamics are described in section 2. In section 3, the enriched basis functions are introduced. Then numerical examples are presented in section 4. Finally, several conclusions are obtained.

2 Dual Hybrid BNM for elastodynamics

As an extension of the Hybrid BNM, the main idea of the Dual Hybrid BNM consists of employing the fundamental solution corresponding to a simpler equation and considering the remaining terms of the original equation via a procedure which involves a series expansion using RBF and the reciprocity principles. For convenience, the body force b_i is set equal to zero, the governing equation for the elastodynamics without damping is written as

$$Gu_{i,kk} + \frac{G}{1-2v} u_{k,ki} = \rho \ddot{u}_i \tag{1}$$

where ρ is density of the material. $G = \frac{E}{2(1+v)}$ is shear modules.

As a consequence, the left-hand side of Eq. 1 can be dealt with Hybrid BNM for the Laplace equation, and the integrals corresponding to the right-hand side are taken to the boundary using DRM. In Dual Hybrid BNM, the solution variables $\mathbf{u}$ can be divided into complementary solutions $\mathbf{u}^c$ and particular solutions $\mathbf{u}^p$, i.e.

$$\mathbf{u} = \mathbf{u}^c + \mathbf{u}^p \tag{2}$$

The particular solution $\mathbf{u}^p$ just needs to satisfy the inhomogeneous equation as follow:

$$Gu^p_{i,kk} + \frac{G}{1-2v} u^p_{k,ki} = \rho \ddot{u}_i \tag{3}$$

The complementary solution $\mathbf{u}^c$ must satisfy the homogeneous equation:

$$Gu^c_{i,kk} + \frac{G}{1-2v} u^c_{k,ki} = 0 \tag{4}$$

and the modified boundary condition:

$$\mathbf{u}^c = \bar{\mathbf{u}}^c = \bar{\mathbf{u}} - \mathbf{u}^p \tag{5}$$

$$\mathbf{t}^c = \bar{\mathbf{t}}^c = \bar{\mathbf{t}} - \mathbf{t}^p \tag{6}$$

where $\bar{\mathbf{u}}$ and $\bar{\mathbf{t}}$ are the prescribed displacements and tractions, respectively.

2.1 Hybrid BNM for Complementary Solutions

The Hybrid BNM is based on a modified variational principle. The functions in the modified principle assumed to be independent are: displacement field u_i within the domain, boundary displacement field $\tilde{u}_i$ and boundary traction $\tilde{t}_i$. Consider a domain Ω enclosed by $\Gamma = \Gamma_u + \Gamma_t$ with prescribed displacement $\bar{u}_i$ and traction

$\bar{t}_i$ at the boundary portions Γ_u and Γ_t, respectively. The corresponding variational function Π_{HB} is defined as

$$\Pi_{HB=}\int_\Omega \frac{1}{2}u_{i,j}C_{ijkl}u_{k,l}\mathrm{d}\Omega-\int_\Gamma \tilde{t}_i(u_i-\tilde{u}_i)\mathrm{d}\Gamma-\int_{\Gamma_t}\bar{t}_i\tilde{u}_i\mathrm{d}\Gamma \tag{7}$$

where, the boundary displacements $\tilde{u}_i$ satisfies the essential boundary condition, i.e. $\tilde{u}_i=\bar{u}_i$ on Γ_u.

With the vanishing of Π_{HB} over the domain and its boundary, the following equivalent integral can be obtained

$$\int_\Gamma (t_i-\tilde{t}_i)\delta u_i\mathrm{d}\Gamma-\int_\Omega \sigma_{ij,j}\delta u_i\mathrm{d}\Omega=0 \tag{8}$$

$$\int_\Gamma (u_i-\tilde{u}_i)\delta\tilde{t}_i\mathrm{d}\Gamma=0 \tag{9}$$

Eq. 8 and Eq. 9 hold for any portion of the domain Ω, for example, a sub-domain Ω_I, defined as an intersection of a domain and a small circle centered at node $\mathbf{s}_I$, and its boundary Γ_I and L_I. (see Fig. 1).

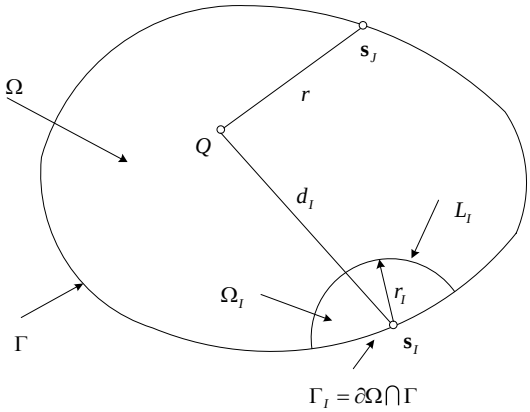

Figure 1: Local domain and source point of fundamental solution corresponding to $\mathbf{s}_I$

We use the following weak form for the sub-domain and its boundary to replace Eq. 8 and Eq. 9

$$\int_{\Gamma_I+L_I}(t_i-\tilde{t}_i)h_I\mathrm{d}\Gamma-\int_{\Omega_I}\sigma_{ij,j}h_I\mathrm{d}\Omega=0 \tag{10}$$

$$\int_{\Gamma_I+L_I}(u_i-\tilde{u}_i)h_I\mathrm{d}\Gamma=0 \tag{11}$$

where $h_I=h_I(Q)$ is a test function. In Eq. 10 and Eq. 11, $\tilde{u}_i$ and $\tilde{t}_i$ at Γ_I can be approximated by the moving least square (MLS) approximation:

$$\tilde{u}(\mathbf{s})=\sum_{J=1}^{N}\Phi_J(\mathbf{s})\hat{u}_J \tag{12}$$

$$\tilde{t}(\mathbf{s})=\sum_{J=1}^{N}\Phi_J(\mathbf{s})\hat{t}_J \tag{13}$$

where N is the number of nodes located on the surface; u_J and t_J are nodal values, and $\Phi_J(\mathbf{s})$ is the shape function of the MLS approximation, corresponding to node $\mathbf{s}_J$ [Miao, Wang, and Yu (2005)].

However, $\tilde{u}_i$ and $\tilde{t}_i$ at L_I has not been defined yet. To solve this problem, we select h_I such that all integrals vanish over L_I. This can be easily accomplished by using the weight function in the MLS approximation for h_I, with the half-length of the major axis d_I of the support of the weight function being replaced by the radius of the sub-domain Ω_I [Miao, Wang, and Yu (2005)]. Therefore, $h_I(Q)$ vanishes on L_I . Eq. 10 and Eq. 11 can be rewritten as

$$\int_{\Gamma_I}(t_i-\tilde{t}_i)h_I\mathrm{d}\Gamma-\int_{\Omega_I}\sigma_{ij,j}h_I\mathrm{d}\Omega=0 \tag{14}$$

$$\int_{\Gamma_I}(u_i-\tilde{u}_i)h_I\mathrm{d}\Gamma=0 \tag{15}$$

$\mathbf{u}$ and $\mathbf{t}$ inside the domain can be approximated by fundamental solutions:

$$\mathbf{u}=\left\{\begin{array}{c}u_1\\u_2\end{array}\right\}=\sum_{J=1}^{N}\left[\begin{array}{cc}u_{11}^J & u_{12}^J\\u_{21}^J & u_{22}^J\end{array}\right]\left\{\begin{array}{c}x_1^J\\x_2^J\end{array}\right\} \tag{16}$$

$$\mathbf{t}=\left\{\begin{array}{c}t_1\\t_2\end{array}\right\}=\sum_{J=1}^{N}\left[\begin{array}{cc}t_{11}^J & t_{12}^J\\t_{21}^J & t_{22}^J\end{array}\right]\left\{\begin{array}{c}x_1^J\\x_2^J\end{array}\right\} \tag{17}$$

where $u_{ij}^J=u_{ij}(\mathbf{s}_J,Q)$ and $t_{ij}^J=t_{ij}(\mathbf{s}_J,Q)$ are the fundamental solutions; x_i^J are unknown parameters.

The final equations can be obtained as

$$\sum_{J=1}^{N}\int_{\Gamma_I}\left[\begin{array}{cc}t_{11}^J & t_{12}^J\\t_{21}^J & t_{22}^J\end{array}\right]\left\{\begin{array}{c}x_1^J\\x_1^J\end{array}\right\}h_I\mathrm{d}\Gamma=\sum_{J=1}^{N}\int_{\Gamma_I}\left[\begin{array}{cc}\Phi_J(\mathbf{s}) & 0\\0 & \Phi_J(\mathbf{s})\end{array}\right]\left\{\begin{array}{c}t_1^J\\t_1^J\end{array}\right\}h_I\mathrm{d}\Gamma \tag{18}$$

$$\sum_{J=1}^{N}\int_{\Gamma_I}\begin{bmatrix} u_{11}^J & u_{12}^J \\ u_{21}^J & u_{22}^J \end{bmatrix}\begin{Bmatrix} x_1^J \\ x_1^J \end{Bmatrix} h_I \mathrm{d}\Gamma = \sum_{J=1}^{N}\int_{\Gamma_I}\begin{bmatrix} \Phi_J(\mathbf{s}) & 0 \\ 0 & \Phi_J(\mathbf{s}) \end{bmatrix}\begin{Bmatrix} u_1^J \\ u_1^J \end{Bmatrix} h_I \mathrm{d}\Gamma \quad (19)$$

Using the above equations for all nodes, one can get the system equations

$$\mathbf{Tx} = \mathbf{H}\hat{\mathbf{t}}^c \quad (20)$$

$$\mathbf{Ux} = \mathbf{H}\hat{\mathbf{u}}^c \quad (21)$$

In the above equations, the elements of **U**, **T** and **H** are given by Miao, Wang, and Yu (2005).

2.2 Dual Reciprocity method (DRM) for Particular Solutions

In the past sections, the complementary solution has been solved successfully by Hybrid BNM, in this section, the DRM will be developed to solve the particular solution.

The DRM can be used in elastodynamic problems to transform the domain integral arising from the application of inhomogeneous into equivalent boundary integrals. Applying interpolation for inhomogeneous term, the following approximation can be proposed for the term $\rho\ddot{u}_i$.

$$\rho\ddot{u}_i \approx \sum_{j=1}^{N+L} f^j \alpha_i^j \quad (22)$$

where α_i^j are a set of initially unknown coefficients, f^j are approximation functions. N and L are the total number of boundary nodes and total number of interior nodes, respectively.

If $\bar{\bar{u}}_{mk}^j$, which called as the basis form of the particular solution, can be found satisfying the following equation:

$$G\bar{\bar{u}}_{mk,ll}^j + \frac{G}{1-2v}\bar{\bar{u}}_{lk,lm}^j = \delta_{mk} f^j \quad (23)$$

Then the particular solution can be approximated by the basis form of the particular solutions. It can be written as following

$$u_i^p \approx \sum_{j=1}^{N+L} \alpha_l^j \bar{\bar{u}}_{li}^j \quad (24)$$

The approximation function f^j can be chosen as $f^j = 1 + r$. Obviously, the basis form of particular solution $\bar{\bar{u}}_{km}$ satisfying Eq. 23 can be obtained as

$$\bar{\bar{u}}_{km} = \frac{1-2v}{(5-4v)G} r_{,m} r_{,k} r^2 + \frac{1}{30(1-v)G}[(3-\frac{10v}{3})\delta_{mk} - r_{,m} r_{,k}] r^3 \quad (25)$$

The corresponding expression for the traction $\bar{\bar{t}}_{km}$ is

$$\begin{aligned}\bar{\bar{t}}_{km} &= \frac{2(1-2\nu)}{5-4\nu}\left[\frac{1+\nu}{1-2\nu}r_{,m}r_{,k}+\frac{1}{2}r_{,k}n_m+\frac{1}{2}\delta_{mk}\frac{\partial r}{\partial n}\right]r \\ &+\frac{1}{15(1-\nu)}\left[(4-5\nu)r_{,k}n_m-(1-5\nu)r_{,m}n_k+\left[(4-5\nu)\delta_{mk}-r_{,m}r_{,k}\right]\frac{\partial r}{\partial n}\right]r^2\end{aligned} \tag{26}$$

And the particular solution of the stress can be given as

$$\begin{aligned}\bar{\bar{\sigma}}_{lkm} &= \frac{2(1-2\nu)}{5-4\nu}\left[\frac{1+\nu}{1-2\nu}\delta_{kl}r_{,m}+\frac{1}{2}(\delta_{mk}r_{,l}+\delta_{ml}r_{,k})\right]r \\ &+\frac{1}{15(1-\nu)}\left[(4-5\nu)(\delta_{mk}r_{,l}+\delta_{ml}r_{,k})-(1-5\nu)\delta_{kl}r_{,m}-r_{,m}r_{,k}r_{,l}\right]r^2\end{aligned} \tag{27}$$

Thus, particular solutions can be written as

$$\mathbf{u}^p = \sum_{I=1}^{N+L}\begin{bmatrix}\bar{\bar{u}}^I_{11} & \bar{\bar{u}}^I_{12}\\ \bar{\bar{u}}^I_{21} & \bar{\bar{u}}^I_{22}\end{bmatrix}\begin{Bmatrix}\alpha^I_1\\ \alpha^I_2\end{Bmatrix} \tag{28}$$

$$\mathbf{t}^p = \sum_{I=1}^{N+L}\begin{bmatrix}\bar{\bar{t}}^I_{11} & \bar{\bar{t}}^I_{12}\\ \bar{\bar{t}}^I_{21} & \bar{\bar{t}}^I_{22}\end{bmatrix}\begin{Bmatrix}\alpha^I_1\\ \alpha^I_2\end{Bmatrix} \tag{29}$$

Substitute Eq. 22 into the Eq. 28 and Eq. 29, one can obtain the particular solution writing in matrix form as

$$\mathbf{u}^p = \rho\mathbf{V}\mathbf{F}^{-1}\ddot{\mathbf{u}} \tag{30}$$

$$\mathbf{t}^p = \rho\mathbf{Q}\mathbf{F}^{-1}\ddot{\mathbf{u}} \tag{31}$$

where vector $\ddot{\mathbf{u}}$ is the value of acceleration on each nodes, and $\mathbf{V}$ and $\mathbf{Q}$ are the matrixes of basic form of particular solution.

For a well-posed problem, either $\tilde{u}_i$ or $\tilde{t}_i$ is known at each node on the boundary. However, transformation between $\hat{u}_i$ and $\tilde{t}_i$, $\hat{t}_i$ and $\tilde{t}_i$ is necessary because the MLS approximation lacks the delta function property. For the faces where $\tilde{u}_i$ is prescribed, $\hat{u}^I_i$ can be computed by

$$\hat{u}^I_i = \sum_{J=1}^{N} R_{ij}\tilde{u}^J_i = \sum_{J=1}^{N} R_{ij}\bar{u}^J_i \tag{32}$$

and for the faces where $\tilde{t}_i$ is prescribed, $\hat{t}^I_i$ can be computed by

$$\hat{t}^I_i = \sum_{J=1}^{N} R_{ij}\tilde{t}^J_i = \sum_{J=1}^{N} R_{ij}\bar{t}^J_i \tag{33}$$

where $R_{IJ} = [\Phi_J(\mathbf{s})]^{-1}$.

Substituting Eqs. (5), (6), (30)- (33) into Eqs. (20) and (21), we can obtain

$$\mathbf{Ux} + \rho\mathbf{HRVF}^{-1}\ddot{\mathbf{u}} = \mathbf{HR}\bar{\mathbf{u}} \tag{34}$$

$$\mathbf{Tx} + \rho\mathbf{HRQF}^{-1}\ddot{\mathbf{u}} = \mathbf{HR}\bar{\mathbf{t}} \tag{35}$$

Solving the coefficient vector $\mathbf{x}$ in (34), one can obtain

$$\mathbf{x} = \mathbf{U}^{-1}\mathbf{HR}(\bar{\mathbf{u}} - \rho\mathbf{VF}^{-1}\ddot{\mathbf{u}}) \tag{36}$$

Then Substitute Eq. 36 into Eq. 35, one can obtain

$$\mathbf{K}\bar{\mathbf{u}} - \mathbf{N}\bar{\mathbf{t}} + \mathbf{K}\ddot{\mathbf{u}} = \mathbf{0} \tag{37}$$

where

$$\mathbf{K} = \mathbf{TU}^{-1}\mathbf{HR}$$

$$\mathbf{N} = \mathbf{HR}$$

$$\mathbf{M} = \rho(\mathbf{HRQF}^{-1} - \mathbf{TU}^{-1}\mathbf{HRVF}^{-1})$$

Eq. 37 is the system equation of the Dual Hybrid boundary node method for dynamic analysis. The system (37) is initially partitioned according to the type of applied boundary conditions, and then statically condensed in such a way that final system could be solved for unknown displacement only. Assuming that N nodes are located on the boundary, we can get N unknown variables on the boundary from Eq. 32. However, the Equation above includes the displacement of the L internal nodes, and so the additional equations are needed.

The unknown variables of the internal nodes can be expressed as

$$\mathbf{u}^* = \mathbf{u}^c + \mathbf{u}^p \tag{38}$$

The complementary solution $\mathbf{u}^c$ can be interpolated by the fundamental solution and the particular solution $\mathbf{u}^p$ can be expressed by Eq. 30. Then Eq. 38 can be rewritten as

$$\mathbf{u}^* = \mathbf{u}^s\mathbf{x} + \rho\mathbf{VF}^{-1}\ddot{\mathbf{u}} \tag{39}$$

where $\mathbf{u}^*$ is the displacement of the internal nodes; $\mathbf{u}^s$ is the matrix of the fundamental solution on each internal nodes; $\mathbf{V}$ is the matrix of values of basis form of particular solution.

Substitute Eq. 36 into Eq. 39, it can be rewritten as

$$\mathbf{u}^* = \mathbf{u}^s\mathbf{U}^{-1}\mathbf{H}\mathbf{R}\bar{\mathbf{u}} - \rho\mathbf{u}^s\mathbf{U}^{-1}\mathbf{H}\mathbf{R}\mathbf{V}\mathbf{F}^{-1}\ddot{\mathbf{u}} + \rho\mathbf{V}\mathbf{F}^{-1}\ddot{\mathbf{u}} \tag{40}$$

Rewrite Eq. 40, one can obtain

$$\mathbf{L}\bar{\mathbf{u}} - \mathbf{I}\mathbf{u}^* + \mathbf{M}_I\ddot{\mathbf{u}} = \mathbf{0} \tag{41}$$

where $\mathbf{I}$ is a unit matrix and

$$\mathbf{L} = \mathbf{u}^s\mathbf{U}^{-1}\mathbf{H}\mathbf{R} \tag{42}$$

$$\mathbf{M}_I = \rho(\mathbf{V}\mathbf{F}^{-1} - \mathbf{u}^s\mathbf{U}^{-1}\mathbf{H}\mathbf{R}\mathbf{V}\mathbf{F}^{-1}) \tag{43}$$

The final system equations are established by combining Eq. 37 and Eq. 41. In this paper, the Newmark time integration scheme is used.

As demonstrated, the Dual Hybrid BNM is a boundary-only meshless approach. No boundary elements are used for both interpolation and integration purpose. The nodes in the domain are needed just for interpolation for the particular solution, which cannot influence the present method as a boundary-type method.

3 Enriched Basis Function

For the two-dimensional fracture problems, the displacement field at the tip of a mixed mode crack is

$$u_1(x) = \frac{K_I}{2G}\sqrt{\frac{r}{2\pi}}\cos\frac{\theta}{2}[\kappa - 1 + 2\sin^2\frac{\theta}{2}] + \frac{K_{II}}{2G}\sqrt{\frac{r}{2\pi}}\sin\frac{\theta}{2}[\kappa + 1 + 2\cos^2\frac{\theta}{2}] \tag{44}$$

$$u_2(x) = \frac{K_I}{2G}\sqrt{\frac{r}{2\pi}}\sin\frac{\theta}{2}[\kappa + 1 - 2\cos^2\frac{\theta}{2}] + \frac{K_{II}}{2G}\sqrt{\frac{r}{2\pi}}\cos\frac{\theta}{2}[\kappa - 1 - 2\sin^2\frac{\theta}{2}] \tag{45}$$

where r is the distance from the point x to the tip of the crack, θ is the angle from the tangent to the crack path at the crack tip (see Fig. 2), G is the shear modulus,

$$\kappa = \begin{cases} 3 - 4v & \text{Plain strain} \\ \dfrac{3-v}{1+v} & \text{Plain stress} \end{cases} \tag{46}$$

and v is the Poisson's ratio.

Meshless approximation can be intrinsically enriched by including the enrichment function in the basis. For fracture problems, one can include the asymptotic near-tip displacement field, or an important ingredient, such as $\sqrt{r}$, in the basis function. The choice of basis functions depends on the coarse-mesh accuracy desired.

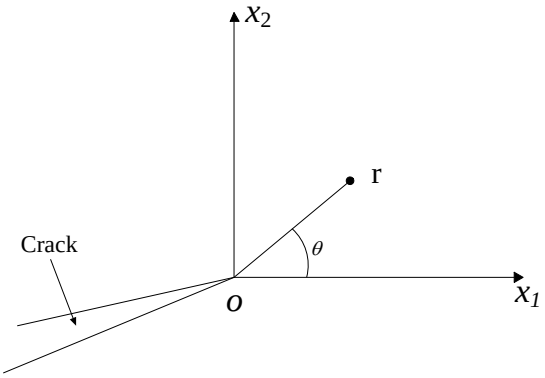

Figure 2: The local coordinate system at the crack tip

To obtain the solution precisely, all terms in the displacement field at the tip of a crack can be included in the basis function. This is the complete enriched basis function method, and the basis function is

$$p^T(x) = [1, x, y, \sqrt{r}\cos\frac{\theta}{2}, \sqrt{r}\sin\frac{\theta}{2}, \sqrt{r}\sin\frac{\theta}{2}\sin\theta, \sqrt{r}\cos\frac{\theta}{2}\sin\theta] \tag{47}$$

For convenience, we also use the local enriched basis function method, and the function $\sqrt{r}$ is used to expand the basis function, i.e.

$$p^T(x) = [1, x, y, \sqrt{r}] \tag{48}$$

Comparing with the complete enriched basis function, the local enriched basis function has greater computing speed, and can simulate the stress field at the tip of a crack well with fewer nodes.

4 Numerical examples

In this section, the Dual Hybrid BNM is implemented and a comprehensive parametric study is conducted to study the dynamic fracture problems. The support size for the weight function d_I is taken to be $3.5h$ in Hybrid BNM, with h being the mesh size. And the parameter c_I is taken to be such that $d_I/c_I = 0.5$, $r_J = 0.8h$ is chosen and the parameter c_I is taken to be $r_I/c_J = 1.1$.

4.1 A circular in an infinite medium with two lateral cracks

The geometry of the problem is shown in Fig. 3. The diameter of the hole is $a = 20mm$ and the distance between both crack tips $d = 60mm$. The material properties

are $E = 76.923GPa$, $v = 0.3$, $\rho = 8000kg/m^3$, and therefore the wave velocities are $c_1 = 5801m/s$ and $c_2 = 3100m/s$. The hole is subjected to an internal pressure p. The time step is $\Delta t = 1\mu s$. 60 nodes are located on the boundary of the hole and 20 nodes per crack. 40 internal nodes are located around the crack in the domain uniformly.

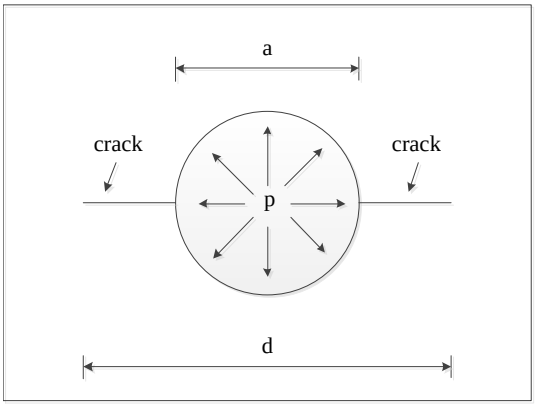

Figure 3: Circular hole under pressure with two lateral cracks

The normalized stress intensity factor (SIF) ($K_I/p\sqrt{\pi a}$) is studied by Dual Hybrid BNM. The example is also studied by Gallego and Dominguez (1996) using hypersingular boundary element method. The comparison of the numerical results using the two methods is presented in Fig. 4. The results show that the proposed approach for SIF evaluation has a good agreement with those of hypersingular BEM. It is simple and produces accurate solutions.

In order to test the sensitivity of the Dual Hybrid BNM to the number of boundary nodes and the number of the internal nodes, different discretizations are applied. For the purpose of error estimation and convergence studies, the relative error is defined as

$$e = \frac{|u^{(n)} - u^{(BEM)}|}{u^{(BEN)}} \tag{49}$$

where the superscripts $u^{(n)}$ and $u^{(BEM)}$ refer to the results of Dual Hybrid BNM and hypersingular BEM. The relative errors for each nodal arrangement in Dual Hybrid BNM computations are presented Fig. 5.

It can be concluded that the more points are arranged in the interior, the more accurate solutions can be obtained from the Fig. 5. It can be observed from this

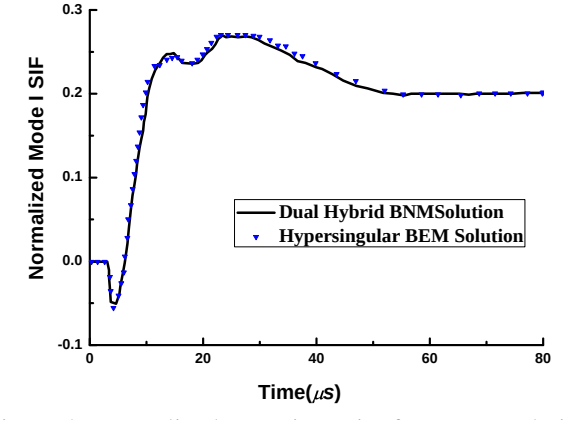

Figure 4: Normalized stress intensity factor at crack tips

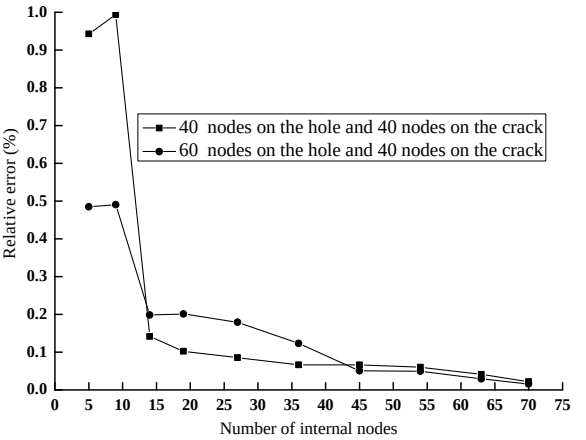

Figure 5: Relative error with different discretizations

figure that the present method gives very good results for this problem when more than 40 internal nodes are used.

4.2 3D Rectangular bar with a central elliptical crack

To verify the feasible of the Dual Hybrid BNM, a three-dimensional dynamic fracture problem is studied. A rectangular bar with cross-section $2a \times 2b$ (as shown in Fig. 6) and height $2h$ contains a centrally located elliptical crack. The dimen-

sions of the bar are $h = 15cm$, $a = 9cm$, $b = 6cm$, the two principal axes of the crack are $c_1 = 3.5cm$ and $c_2 = 1.5cm$. The material constants are: bulk modulus $K = 165GPa$, shear modulus $G = 77GPa$ and density $\rho = 7.9mg/m^3$. The bar is subjected to a Heaviside load $\sigma_0 H(t)$ on the ends. The total number of collocation nodes is 360 on the boundary of the bar and 180 nodes on the boundary of the crack. There are 360 nodes in the domain for RBF interpolation.

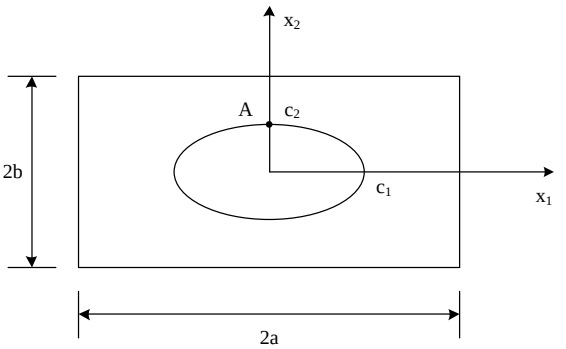

Figure 6: Elliptical Crack

The normalized dynamic stress intensity factor at the end of the minor axis is plotted, as $\sqrt{\pi}K_I(t)/\sigma_0$, against real time $t(\mu s)$ in Fig. 7. The numerical example is also studied by Wen, Aliabadi, and Rooke (1999b) using DRM in Laplace domain. The numerical results given by DRM in time domain [Wen, Aliabadi, and Rooke (1999a)] and in Laplace domain are shown in the same figure with those from the presented method, which shows good general agreement.

4.3 Rectangular plate with an inclined surface crack

To demonstrate the capability of the present method, a mixed mode problem has been studied. A rectangular plate, as shown in Fig. 8, contains a crack inclined 45° from the boundary loaded by a uniform end tension σ applied at $t = 0$ with a Heaviside-function time dependence. This problem was studied by the researchers [Murti and Valliappan (1986); Aoki, Kishimoto, Izumihara, and Sakata (1980)] using singular finite element method. The dimension of the problem is shown in Fig. 8. The material properties are: shear modulus $G = 29.4GPa$, Poisson's ratio $v = 0.286$ and the density $\rho = 2450kg/m^3$.

In the present calculation, the boundary of the quadrant of the plate is divided into seven piecewise smooth segments. 80 boundary nodes are located on the boundary

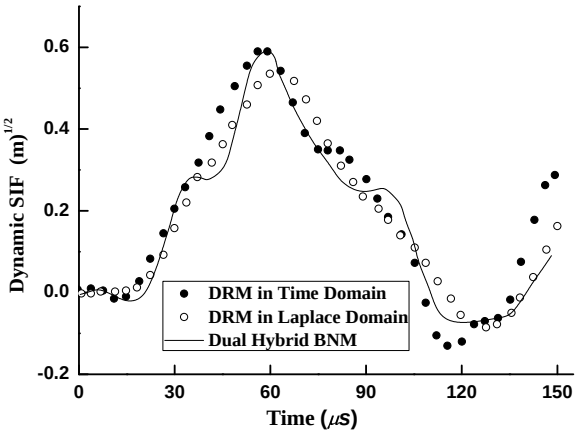

Figure 7: Normalized stress intensity factor for rectangular bar containing an elliptical crack

of the rectangular plate and 10 boundary nodes on crack uniformly. 64 internal nodes are located in the domain uniformly.

The Newmark method is used with $\Delta t = 0.5\mu s$ and results are computed till $t = 25\mu s$. The results of the normalized mode I and mode II stress intensity factors for the plate with an inclined surface crack were shown in Fig. 9 and Fig. 10, in which the singular FEM solutions are also in the graph. It can be seen from the results that the Dual Hybrid BNM solutions are close to the singular FEM results.

5 Conclusions

In this paper, the Dual Hybrid BNM for dynamic fracture problems is developed. This method combines the DRM and Hybrid BNM. The Hybrid BNM is used to solve the homogeneous equations, while the DRM is employed to solve the inhomogeneous terms. No cells are needed either for the interpolation purposes or for integration process, only discrete nodes are constructed on the boundary of a domain, several nodes in the domain are needed just for the RBF interpolation. In order to simulate the singularity of the stress on the crack tip, enriched basis functions are used.

The internal nodes used in the present method are usually defined at positions where the solution is required. The use of a number of internal nodes is important in most cases. Based on the numerical examples, the number of internal node $L = N/2$, where N is the number of boundary nodes, provides solutions which are satisfactory

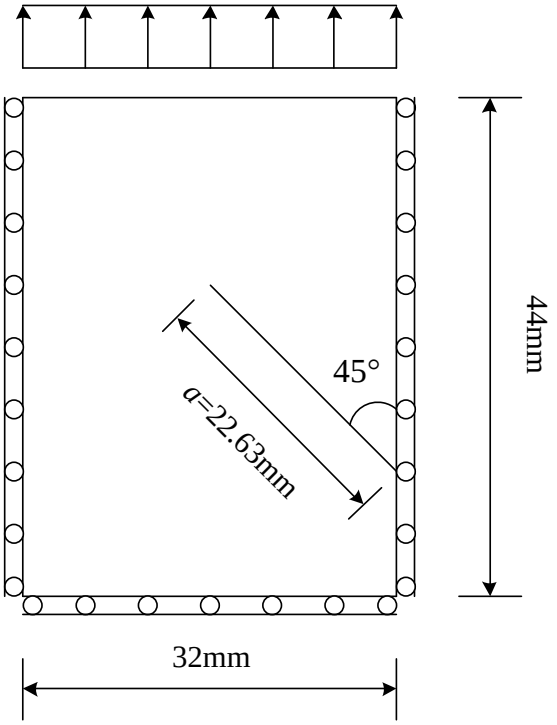

Figure 8: Rectangular plate with an inclined surface crack

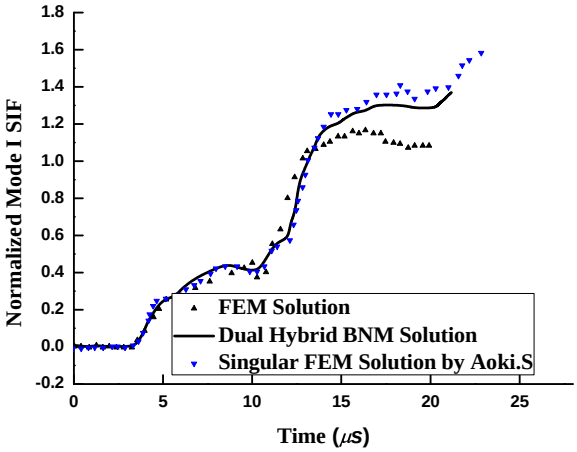

Figure 9: Normalized Mode I SIF versus time

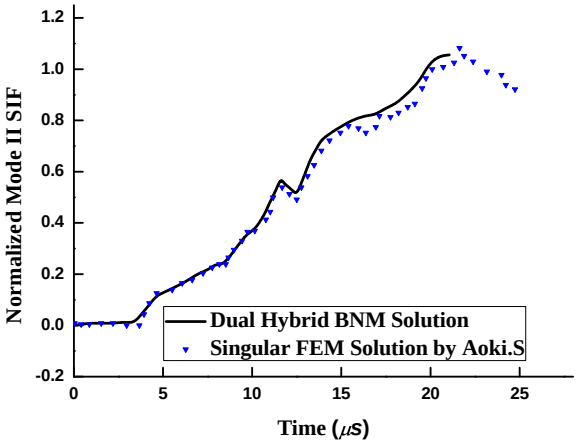

Figure 10: Normalized Mode II SIF versus time

for all problems.

The method here developed represents a very promising alternative to solving dynamic fracture propagation problems. Only discrete nodes are arranged on the faces of the crack, which simplifying greatly the remeshing process with respect to what is necessary in domain numerical techniques.

Acknowledgement: Financial support for the project from the National Basic Research Program of China (973 Program: 2011CB013800) and the Natural Science Foundation of China (No. 50808090).

References

Aoki, S.; Kishimoto, K.; Izumihara, Y.; Sakata, M. (1980): Dynamic analysis of cracked linear viscoelastic solids by finite element method using singular element. *International Journal of Fracture*, vol. 16, no. 2, pp. 97–109.

Atluri, S.; Zhu, T. (1998): A new meshless local petrov-galerkin (mlpg) approach in computational mechanics. *Computational mechanics*, vol. 22, no. 2, pp. 117–127.

Belytschko, T.; Lu, Y.; Gu, L. (1994): Element-free galerkin methods. *International journal for numerical methods in engineering*, vol. 37, no. 2, pp. 229–256.

Budreck, D. E.; Achenbach, J. D. (1988): Scattering from three-dimensional planar cracks by the boundary integral equation method. *Journal of Applied Mechanics*, vol. 55, no. 2, pp. 405–412.

Dolbow, J.; Moës, N.; Belytschko, T. (2000): Discontinuous enrichment in finite elements with a partition of unity method. *Finite Elements in Analysis and Design*, vol. 36, no. 3, pp. 235–260.

Dominguez, J.; Gallego, R. (1992): Time domain boundary element method for dynamic stress intensity factor computations. *International journal for numerical methods in engineering*, vol. 33, no. 3, pp. 635–647.

Gallego, R.; Dominguez, J. (1996): Hypersingular bem for transient elastodynamics. *International journal for numerical methods in engineering*, vol. 39, no. 10, pp. 1681–1705.

Hirose, S.; Achenbach, J. (1989): Time-domain boundary element analysis of elastic wave interaction with a crack. *International journal for numerical methods in engineering*, vol. 28, no. 3, pp. 629–644.

Li, S.; Cheng, Y. (2005): Enriched meshless manifold method for two-dimensional crack modeling. *Theoretical and applied fracture mechanics*, vol. 44, no. 3, pp. 234–248.

Liu, G.; Gu, Y. (2001): A local radial point interpolation method (lrpim) for free vibration analyses of 2-d solids. *Journal of Sound and Vibration*, vol. 246, no. 1, pp. 29–46.

Miao, Y.; Wang, Y. (2006): Meshless analysis for three-dimensional elasticity with singular hybrid boundary node method. *Applied Mathematics and Mechanics*, vol. 27, no. 5, pp. 673–681.

Miao, Y.; Wang, Y.; Wang, Y. (2009): A meshless hybrid boundary-node method for helmholtz problems. *Engineering analysis with boundary elements*, vol. 33, no. 2, pp. 120–127.

Miao, Y.; Wang, Y.; Yu, F. (2005): Development of hybrid boundary node method in two-dimensional elasticity. *Engineering analysis with boundary elements*, vol. 29, no. 7, pp. 703–712.

Moës, N.; Belytschko, T. (2002): Extended finite element method for cohesive crack growth. *Engineering Fracture Mechanics*, vol. 69, no. 7, pp. 813–833.

Moës, N.; Dolbow, J.; Belytschko, T. (1999): A finite element method for crack growth without remeshing. *International Journal of Numerical Methods in Engineering*, vol. 46, pp. 131–150.

Mukherjee, Y.; Mukherjee, S. (1997): The boundary node method for potential problems. *International Journal for Numerical Methods in Engineering*, vol. 40, no. 5, pp. 797–815.

Murti, V.; Valliappan, S. (1986): The use of quarter point element in dynamic crack analysis. *Engineering Fracture Mechanics*, vol. 23, no. 3, pp. 585–614.

Nardini, D.; Brebbia, C. (1983): A new approach to free vibration analysis using boundary elements. *Applied mathematical modelling*, vol. 7, no. 3, pp. 157–162.

Rao, B.; Rahman, S. (2004): An enriched meshless method for non-linear fracture mechanics. *International Journal for Numerical Methods in Engineering*, vol. 59, no. 2, pp. 197–223.

Wen, P.; Aliabadi, M.; Rooke, D. (1999): A mass-matrix formulation for three-dimensional dynamic fracture mechanics. *Computer methods in applied mechanics and engineering*, vol. 173, no. 3, pp. 365–374.

Wen, P.; Aliabadi, M.; Rooke, D. (1999): Three-dimensional dynamic fracture analysis with the dual reciprocity method in laplace domain. *Engineering analysis with boundary elements*, vol. 23, no. 1, pp. 51–58.

Zhang, J.; Yao, Z. (2001): Meshless regular hybrid boundary node method. *CMES: Computer Modeling in Engineering and Sciences*, vol. 2, no. 3, pp. 307–318.

Zhang, J.; Yao, Z. (2004): The regular hybrid boundary node method for three-dimensional linear elasticity. *Engineering analysis with boundary elements*, vol. 28, no. 5, pp. 525–534.

Zhang, J.; Yao, Z.; Li, H. (2002): A hybrid boundary node method. *International Journal for Numerical Methods in Engineering*, vol. 53, no. 4, pp. 751–763.